ResearchGate

See discussions, stats, and author profiles for this publication at: https://www.researchgate.net/publication/23784198

A Soft Preparative Method for Membrane Proteome Analysis Using Frit Inlet Asymmetrical Flow Field−Flow Fractionation: Application in a Prostatic Cancer Cell Line

ARTICLE *in* JOURNAL OF PROTEOME RESEARCH · FEBRUARY 2009

Impact Factor: 4.25 · DOI: 10.1021/pr800689y · Source: PubMed

CITATIONS
13

READS
33

4 AUTHORS, INCLUDING:

Dukjin Kang
Korea Research Institute of Standards and …
28 PUBLICATIONS **454** CITATIONS
SEE PROFILE

Jong Shin Yoo
Korea Basic Science Institute KBSI
194 PUBLICATIONS **3,471** CITATIONS
SEE PROFILE

Myeong Hee Moon
Yonsei University
150 PUBLICATIONS **2,417** CITATIONS
SEE PROFILE

Available from: Jong Shin Yoo
Retrieved on: 31 January 2016

Journal of proteome research

Subscriber access provided by YONSEI UNIV

Article

A Soft Preparative Method for Membrane Proteome Analysis Using Frit Inlet Asymmetrical Flow Field-Flow Fractionation: Application in a Prostatic Cancer Cell Line

Dukjin Kang, Jong Shin Yoo, Myeong Ok Kim, and Myeong Hee Moon

J. Proteome Res., **2009**, 8 (2), 982-991 • DOI: 10.1021/pr800689y • Publication Date (Web): 13 January 2009

Downloaded from http://pubs.acs.org on February 8, 2009

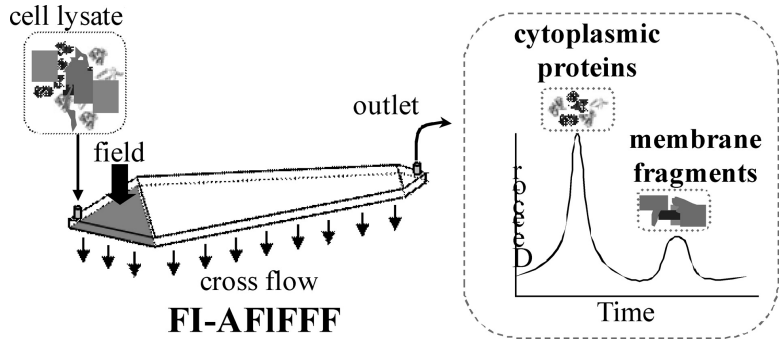

More About This Article

Additional resources and features associated with this article are available within the HTML version:

- Supporting Information
- Access to high resolution figures
- Links to articles and content related to this article
- Copyright permission to reproduce figures and/or text from this article

View the Full Text HTML

ACS Publications
High quality. High impact.

Journal of Proteome Research is published by the American Chemical Society.
1155 Sixteenth Street N.W., Washington, DC 20036

research articles Journal of proteome research

A Soft Preparative Method for Membrane Proteome Analysis Using Frit Inlet Asymmetrical Flow Field-Flow Fractionation: Application in a Prostatic Cancer Cell Line

Dukjin Kang,[†,‡] Jong Shin Yoo,[*,‡] Myeong Ok Kim,[§] and Myeong Hee Moon[*,†]

Department of Chemistry, Yonsei University, Seoul, 120-749, South Korea, Mass Spectrometry Research Center, Korea Basic Science Institute, Ochang, Chungcheongbuk-Do, 363-883, South Korea, and Division of Life Science and Applied Life Science (BK21), Gyeongsang National University, Jinju, 660-701, South Korea

Received August 31, 2008

Membrane proteins participate in a number of important biological functions such as signal transduction, molecular transport, and cell−cell interactions. However, due to the nature of membrane proteins, the development of a preparative method that produces a sufficient yield of purified membrane proteins from the cell remains a challenge. In the present study, frit inlet asymmetrical flow field-flow fractionation (FI-AFlFFF) was employed to fractionate membrane fragments containing membrane proteins from free cytoplasmic proteins of prostatic cancer cell (DU145 cell) lysates. The isolated membrane proteins were then digested and analyzed by nanoflow liquid chromatography/tandem mass spectrometry (nLC-ESI-MS-MS). Since fractionation of the cell lysate mixtures containing membrane fragments and cytoplasmic proteins could be achieved based on the differences of their sizes in FI-AFlFFF, membrane fragments were partially isolated from the cytoplasmic proteins and collected. The performance of FI-AFlFFF for prefractionation of the membrane proteome was examined by comparing the number of membrane proteins that were identified with the number identified using an ultracentrifugation method. The application of FI-AFlFFF to membrane proteomics produced an increased yield of purified membrane proteins with fewer cytoplasmic proteins compared to a conventional ultracentrifugation method.

Keywords: frit-Inlet asymmetrical field-flow fractionation • FlFFF • membrane fractionation • membrane proteomics • 2D-LC-ESI-MS-MS • mass spectrometry

Introduction

The field of membrane proteomics attempts to understand the biological function of the membrane and its signaling pathways in relation to human disease and pathogenesis. Recent studies have revealed a number of critical roles of specific membrane proteins that regulate cell longevity, necrosis, and death.[1−3] A systematic understanding of the functions of the membrane proteome may potentially provide keys to uncover diagnostics for human diseases, signaling receptors, and therapeutic solutions.[4] Despite its promise, however, profiling of membrane proteomes is challenging because of several difficulties and limitations innate to its analysis, specifically, the low abundance of membrane proteins, the lack of a proper preparative method to completely separate cytoplasmic proteins from membrane proteins, and limited options for proteolytic enzymes. Moreover, the poor solubility of membrane proteins adds an additional barrier to conventional gel-based techniques.[4,6,7]

Ultracentrifugation, a traditional preparative tool in biological studies, is widely utilized for the purification of membrane proteins from cells and is based on well-established protocols. However, ultracentrifugation has several drawbacks, including low yield and reproducibility, since it often requires repeated purification steps to deplete cytoplasmic proteins and/or other impurities. In addition, the formation of pellets of membrane debris at the bottom surface of centrifugal tube has been shown to reduce the efficiency of proteolytic cleavage.[8,9]

Flow field flow fractionation (FlFFF), an elution-based separation technique, can alternatively be utilized as a soft preparative method for isolating membrane proteins. Indeed, FlFFF has become a universal tool for separating and characterizing macromolecules, colloids, water-soluble polymers, and nano- to micron-sized particles.[10−12] Very recently, we reported on a powerful application of FlFFF, whereby it can be employed as a tool to complement conventional density gradient centrifugation methods for characterizing size-dependent proteome pattern of biological vesicles and organelles such as mitochondria and exosomes.[13−15] In FlFFF, separation of particles or proteins is carried out in a thin and unobstructed rectangular channel via the application of a crossflow as an external field to retain sample components, which acts across the channel thickness; this occurs in addition to a migration flow which moves along the axis of the channel. Figure 1a

* To whom correspondence should be addressed. Myeong Hee Moon, Department of Chemistry Yonsei University Seoul, 120-749, Korea. Phone: (82) 2.2123.5634; fax, (82) 2 364.7050; e-mail, mhmoon@yonsei.ac.kr
† Yonsei University.
‡ Korea Basic Science Institute.
§ Gyeongsang National University.

10.1021/pr800689y CCC: $40.75
© 2009 American Chemical Society
Published on Web 01/13/2009

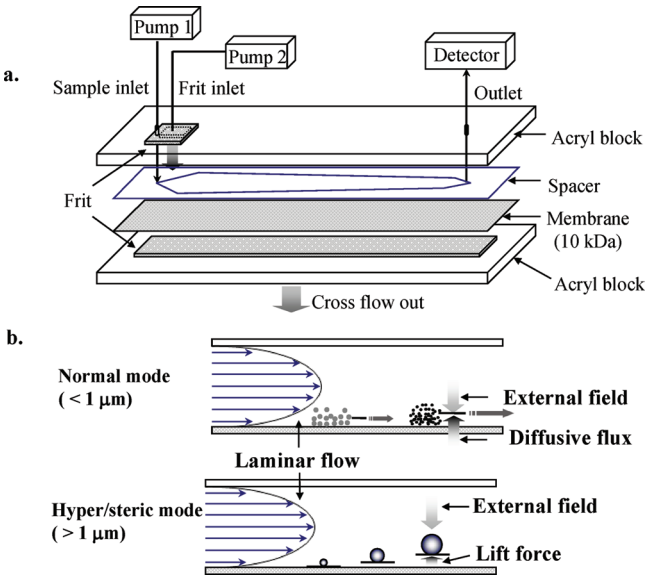

Figure 1. (a) System configuration of frit-inlet asymmetrical flow field-flow fractionation (FI-AFlFFF) and (b) a side view of the FI-AFlFFF channel showing the two opposite elution mechanisms (hyperlayer and normal modes) depending on particle size.

Scheme 1. Experimental Scheme for Membrane Proteome Analysis of DU145 Cells for Two Different Purification Methods: FI-AFlFFF and Ultracentrifugation

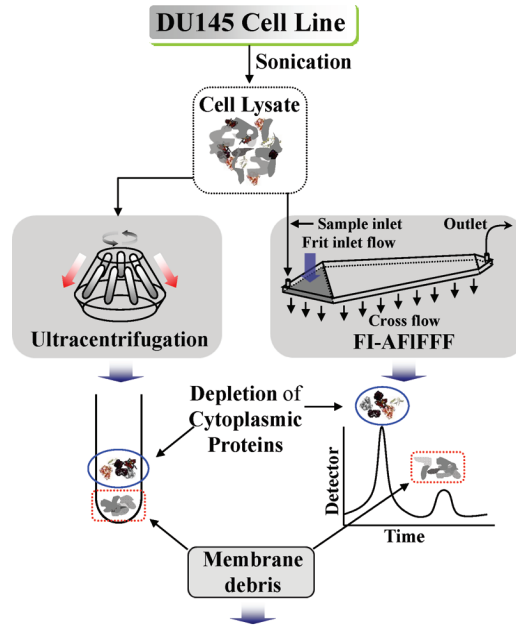

illustrates the structure of a modified FlFFF channel utilized in this study, which follows the same basic principles of FlFFF separation as described above. Proteins under an external field (crossflow in FlFFF) are driven toward one wall of the FlFFF channel (referred to as the accumulation wall) that is composed of a porous frit that allows the crossflow to pass through and a channel membrane, which is layered above the frit, to prevent the sample components from passing through. At the same time, the sample components (particles or proteins) are elevated from the accumulation wall based on their size due to diffusion. More specifically, due to the differences in the diffusive forces of the sample components, smaller sized components are elevated further away from the accumulation wall relative to larger components. Thus, sample materials are differentially distributed across the channel thickness depending on the balance of the two counter-directing forces (crossflow and diffusion). When a laminar flow is applied along the channel axis for sample migration, the smaller proteins that are entrained in the faster flowing laminar in the FlFFF channel elute first compared to larger ones (referred to as "normal mode", as shown in Figure 1b).[16] Therefore, separation is achieved at an increasing order of diffusion coefficients or hydrodynamic diameters. For supramicrometer-sized particles or cells, however, diffusion forces are relatively negligible and the hydrodynamic sizes of sample components become the main factor controlling particle protrusion into the laminar flow streamlines. In such a case, retention of supramicrometer-sized cells follows the steric/hyperlayer mode in which large particles or cells protrude toward the faster streamlines of the laminar flow due to the size effect, and thus, the larger cells elute earlier than smaller ones. These two separation mechanisms are illustrated in Figure 1b.

In this study, we utilized FlFFF as a potential alternative method for the simultaneous isolation and purification of membrane fragments from cell lysates in order to characterize membrane proteins. We compared this new technique with that of conventional centrifugation methods for membrane purification. Cell lysates from the prostatic cancer cell line (DU145) were directly fractionated by FlFFF using a frit inlet asymmetrical channel[14,18,19] for the collection of membrane fragments containing membrane proteins, which were differentiated from free, unbound cytoplasmic proteins on the basis of retention time. For a comparison study, membrane fragments were also purified using a conventional ultracentrifugation method with triplicate purification cycles to achieve cytoplasmic protein depletion. Both the fractions from FlFFF and ultracentrifugation were further lysed, tryptically digested, and the resulting purified peptide mixtures were analyzed by online two-dimensional strong-cation exchange−reversed-phase liquid chromatography−electrospray ionization−tandem mass spectrometry (2D-SCX-RPLC-ESI-MS-MS) for protein identification. The experimental schemes for the comparative study are illustrated in Scheme 1. The efficiencies of the methods were evaluated by comparing the number of membrane proteins identified by FlFFF with that of ultracentrifugation.

Materials and Methods

Culture and Lysis of the DU145 Cell Line. The prostatic DU145 (human HRPC cell line) cell line was obtained from the Korea Cell Line Bank (KCLB, Seoul). DU145 cells were grown in triplicate culture plates containing RPMI-1640 (HyClone, Logan, UT) and maintained in a humidified atmosphere containing 5% CO_2 at 37 °C for 72 h. Media was supplemented with 10% heat-inactivated fetal bovine serum (Gibco; Grand Island, NY), 1% antibio-antimicotic solution containing 10 000 units/mL penicillin, and 10 mg/mL each of streptomycin (HyClone; Logan, UT), HEPES, sodium bicarbonate, *p*-aminobenzoic acid, and insulin. Next, the cells were subcultured (the standard concentration of cells was 1×10^5/mL for each cell line) with the respective culture media in 60 mm plates (Nunc; Denmark) under the same conditions as described above, but for a shorter period of 24 h. All other chemicals used in the work were purchased from Sigma (St. Louis, MO). DU145

cells were harvested after 24 h of culturing.[17] To remove the detergents and culture media that may have otherwise impeded the enzymatic digestion of membrane proteins, the harvested cells were resuspended with a 10 mM NH_4HCO_3 solution and then centrifuged twice for 10 min at 1000*g* through a 10 kDa molecular weight cutoff (MWCO) Microcon YM-10 filter (Millipore; Danvers, MA) to an approximate volume of 1.0 mL. After resuspending the cells in 10 mM NH_4HCO_3, the cells were lysed by tip-sonication in an ice-cold bath for 1 min and the resulting mixtures were used directly for both FlFFF and ultracentrifugation for the isolation of membrane fragments.

For the purification of membrane fragments by ultracentrifugation, which was performed in order to form a basis for comparison to FlFFF, part of the cell lysate mixtures described above were subjected to conventional ultracentrifugation at 100 000*g* and 4 °C for 60 min. To deplete cytoplasmic proteins from the membrane fragments, the retrieved membrane pellets obtained from first purification process were resuspended in a 10 mM NH_4HCO_3 solution at 4 °C for ultracentrifugation; this process was repeated twice thereafter. All membrane fractions obtained from the ultracentrifugation method were stored at − 80 °C prior to their use.

FlFFF. For FlFFF separation of membrane fragments from cell lysates, a frit inlet asymmetrical flow field-flow fractionation (FI-AFlFFF) channel was utilized. The FI-AFlFFF channel was a modified form of the asymmetrical FlFFF channel detailed in several of our previous studies;[14,18,19] the structure of the FI-AFlFFF channel is illustrated in Figure 1. Briefly, the FI-AFlFFF channel was similar to a conventional asymmetrical FlFFF channel, with the exception that it had a small sized frit placed in the sample inlet area of the depletion wall (opposite to the accumulation wall). In the FI-AFlFFF channel, sample relaxation was achieved hydrodynamically by the application of high speed frit flow through the inlet frit to the incoming sample components from the channel inlet. Therefore, sample injection-relaxation-migration could be achieved smoothly without the need to stop migration flow, as is often required by conventional FlFFF systems. The channel space of the FI-AFlFFF system used in this study was made by cutting a 170 μm thick Mylar sheet into a 27.2 cm long (a tip-to-tip length, L_{tt}) piece with an initial channel breadth of 2.0 cm that decreased to a final breadth of 1.0 cm, thus, forming a trapezoid. The geometrical void volume of the FFF channel was 0.66 mL. At the accumulation wall, a sheet membrane, a model PLCGC (MWCO: 10 kDa) (Millipore Corp.; Danvers, MA), was placed above the frit to keep sample materials from penetrating the accumulation wall.

For FlFFF separation of the cell lysate, a 0.1 M solution of phosphate buffered saline (PBS; pH 7.6), which was first filtered through a 0.45 μm membrane, was used as a carrier solution. For separation, 25 μL of the lysate sample was initially injected into the channel using a model 7125 loop injector from Rheodyne (Cotati, CA). To collect a sufficient quantity membrane fragments, injections were repeated 20 times, and thus, 0.5 mL of lysates were fractionated in total. The cell lysates and carrier solution were delivered to the channel inlet and frit inlet, respectively, by two model 930 HPLC pumps from Young-Lin Co. (Seoul, Korea). For flow optimization of FI-AFlFFF separation, a model Whitey SS-22RS2 metering valve from Crawford Fitting Co. (Solon, OH) was placed after the detector to provide back-pressure and regulate flow rates. When collecting fractions of membrane fragments by FI-AFlFFF, a fused silica capillary tubing (100 μm-i.d.; 360 μm-o.d.) was connected at the outlet of the UV detector with a length adjustment in order to achieve the desired outflow rate. Eluted cell lysate fractions were detected using a model 730 UV detector from Young-Lin Co. (Seoul, Korea) set at a wavelength of 254 nm; detector signals were recorded with Autochro-Win software from Young-Lin.

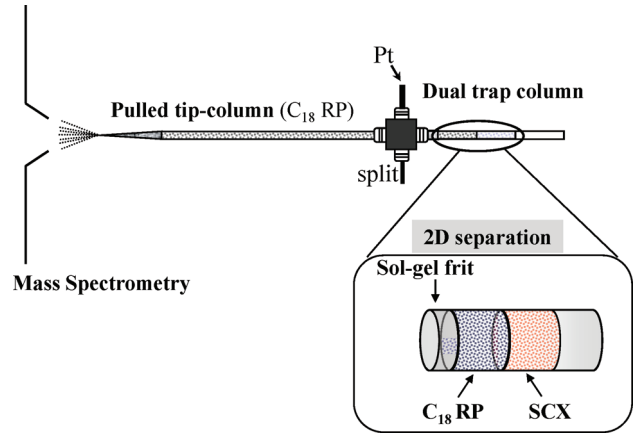

Figure 2. Schematics of the online 2D-SCX-LC setup for ESI-MS-MS using a dual sample trap sequentially packed with RP and SCX resins.

To analyze the performance of FI-AFlFFF separation of intact cells, polystyrene latex (PS) standards (Duke Scientific Co., Palo Alto, CA) with nominal diameter values of 20, 10, 7, and 5 μm were utilized. The carrier solution, which was used only for the separation of PS standards, was a 0.05% sodium dodecylsulfate (SDS) solution supplemented with 0.02% NaN_3 as a bactericide.

In-Solution Digestion. Prior to proteolytic cleavage, the collected fractions from both the FI-AFlFFF and ultracentrifugation methods were examined to calculate protein concentrations by the Bradford assay. Thereafter, all fractions were digested simultaneously under the same conditions and procedures. Specifically, membrane fractions from each preparative method were washed sequentially with ice-cold 0.1 M ammonium carbonate (pH 11) solution, dissolved in 1 mL of formic acid (90%), and digested with CNBr from Sigma (St. Louis, MO) for 24 h at room temperature. After this first proteolytic step, the volume of each fraction was reduced to approximately 200 μL and the pH of each solution was adjusted to 8.6 with solid ammonium carbonate and 1 M urea. Finally, each fraction was digested with trypsin for 24 h at 37 °C. After the proteolytic cleavage step was complete, undigested membrane proteins and fragments were removed using a 3 kDa MWCO Microcon YM-3 filter from Millipore (Danvers, MA).[5]

Two-Dimensional Nanoflow LC-ESI-MS-MS. Two-dimensional nLC-ESI-MS-MS was carried out using a model 1200 microflow HPLC system from Agilent Technologies (Palo Alto, CA) interfaced with an LCQ Deca Max ion-trap mass spectrometer from Thermo Finnigan (San Jose, CA) via electrospray ionization. Peptide mixtures of each fraction from the enzymatic cleavage step were separated using online two-dimensional nanoflow strong-cation exchange−reversed-phase liquid chromatography (SCX-RPLC), which was performed using a homemade dual purpose sample trap (SCX and RP resins) equipped with an analytical capillary RPLC column (170 mm × 75 μm) that was also prepared in our laboratory. Schematics of the dual trap online nanoflow 2D (SCX-RP) LC are shown in Figure 2; details can be found in our previous studies.[14,20] The pulled tip capillary column used in this study was directly packed in our laboratory with Magic C_{18}AQ (3 μm, 100 Å) resin

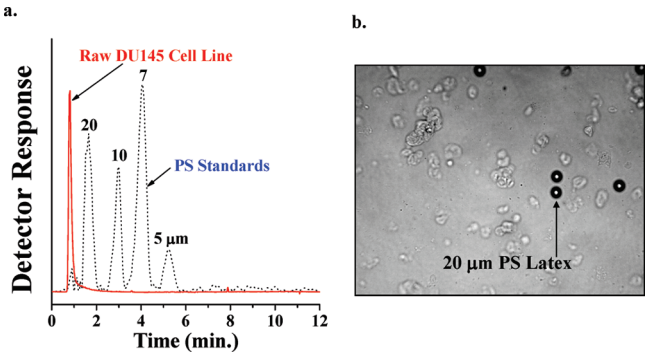

Figure 3. (a) Superimposed FI-AFlFFF fractograms of intact DU145 cells (solid line) and polystyrene standards (dotted line) obtained under the same flow rate conditions: sample flow/outflow rates = 0.1/0.2 mL/min and frit inlet flow/crossflow rates = 2.0/1.9 mL/min; (b) an optical micrograph of the mixtures of DU145 cells and PS 20 μm standards.

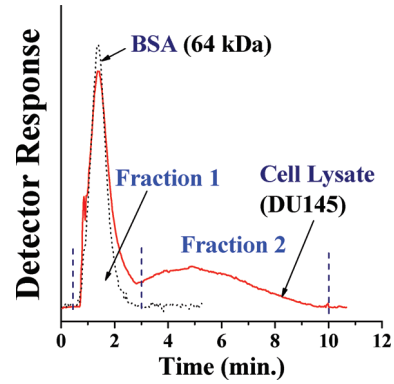

Figure 4. FI-AFlFFF fractograms of cell lysates (solid line) and BSA (dotted line) obtained under the same run conditions used in Figure 3, along with fractions collected at time intervals of 0 ~ 3, 3 ~ 10 min for secondary analysis with online 2D-SCX-LC-MS-MS.

purchased from Michrom BioResources, Inc. (Auburn, CA). Before packing, one end of the capillary tubing was pulled by flame to make the tip like a needle, with an i.d. of approximately ~10 μm. The dual trap column was prepared in a capillary (200 μm−i.d., 360 μm−o.d.) equipped with an end frit (2 mm in length) via sol−gel polymerization at one end of capillary. Afterward, the capillary was packed in sequence with Magic C_{18}AQ (5 μm, 200 Å) resins for the first 0.7 cm and Polysulfethyl A, a strong-cation exchange resin (5 μm, 300 ang), from The Nest Group, Inc. (Southboro, MA) for the final 1.3 cm. The dual trap column and the analytical column were connected via a PEEK microcross as shown in Figure 2. A platinum wire was used as an electrode.

For 2D SCX-RPLC separation, nine salt steps of solutions of 0, 5, 8, 10, 15, 20, 50, 100, and 1000 mM NH_4HCO_3 were used to fractionate the peptide mixture from the SCX trap to the RP portion of the dual trap column, and after each salt step elution, a binary gradient RPLC run was performed. For RPLC runs, two buffer solutions, namely, (A) 2% ACN or (B) 95% ACN in water, both with 0.1% formic acid, were used as mobile phase solutions. The flow rate for the RPLC runs was 200 nL/min and the binary gradient run conditions were as follows: buffer B increased from 0 to 8% for 12 min, followed by a linear increase to 18% over a period of 5 min, 32% over 60 min, then ramped to 80% over 3 min, and finally held at 80% for 10 min to clean the RP column. The column was then decreased to 0% B and held there for 20 min to re-equilibrate the column.

The eluted peptides from capillary column were fed directly into an ion trap mass spectrometer via electrospray ionization in positive ion mode, where a voltage of 2.0 kV was applied through the Pt wire connected to the microcross. MS analysis was carried out by each precursor scan (300−1800 amu) followed by three data-dependent MS-MS scans. MS-MS spectra were analyzed using Bioworks Browser software (Ver 3.2 EF 2) from Thermo-Finnigan against a human database from NCBI. The mass tolerance between the measured monoisotopic mass and the calculated mass was 1.5 and 1.0 u for the molar mass of a precursor peptide and the mass of the peptide fragment ions, respectively. To increase the validity of our search results, identified proteins were selected only if the following requirements were met: A ΔCn score of 0.1 and cross-correlation (Xcorr) values larger than 2.3, 2.8, and 3.5 for singly-, doubly-, and triply charged ions, respectively. Homoserine lactones of methionine, including variable modifications such as oxidation of methionine, tryptic enzyme products, and double miscleavages, were defined.

Result and Discussion

With the use of FI-AFlFFF, cell lysates were fractionated into different sizes, although only two different size fractions were obtained from the 20 repeated batch injections. This was due to the limited throughput of the current channel system. Each injection volume of cell lysate was 25 μL, and thus, a total of 0.5 mL of lysate was fractionated without any washing treatments. Throughput could have been increased if the FI-AFlFFF channel scale had been enlarged; however, an ordinary scale channel was sufficient for the needs of the present method evaluation study. Membrane fragments collected from both FI-AFlFFF and ultracentrifugation methods were processed using the same proteomic analysis method. The enzymatic cleavage was followed by shotgun analysis of peptide mixtures of each fraction by 2D-SCX-LC-MS-MS in order to identify components of the membrane proteome.

Before fractionating membrane fragments with FI-AFlFFF, the flow rate conditions were examined with four PS standards having diameters of 20, 10, 7, and 5 μm in order to achieve conditions for which the supramicrometer-sized cells would separate. Since the diameters of the DU145 cells are larger than a few micrometers, intact cells are expected to elute in the steric/hyperlayer mode. Figure 3a shows the two superimposed fractograms of intact DU145 cells (solid line) and PS standards (dotted line), respectively. The two fractograms were obtained under the same flow rate conditions: the sample inlet and outlet flow rates were 0.1 and 0.2 mL/min, and frit inlet and cross-flow rates were 2.0 and 1.9 mL/min, respectively. The fractogram of PS standards showed a hyperlayer elution of particles with a decreasing order of diameters, demonstrating that the flow rate conditions of FI-AFlFFF were suitable for the size sorting of micromer-sized particles. Under the same flow rate condition, injection of intact DU145 cells yielded a sharp peak that eluted earlier than the 20 μm PS standard, indicating that the cell diameters were larger than ~20 μm in their intact conditions. Further, as shown in the micrograph of intact cells mixed with 20 μm PS in Figure 3b, some of the DU145 cells appeared to be larger than 20 μm. Since the shape of the DU145 cells are not spherical, they are expected to have extra hydrodynamic lift forces and thus should be pushed further away from the channel such that they elute earlier than

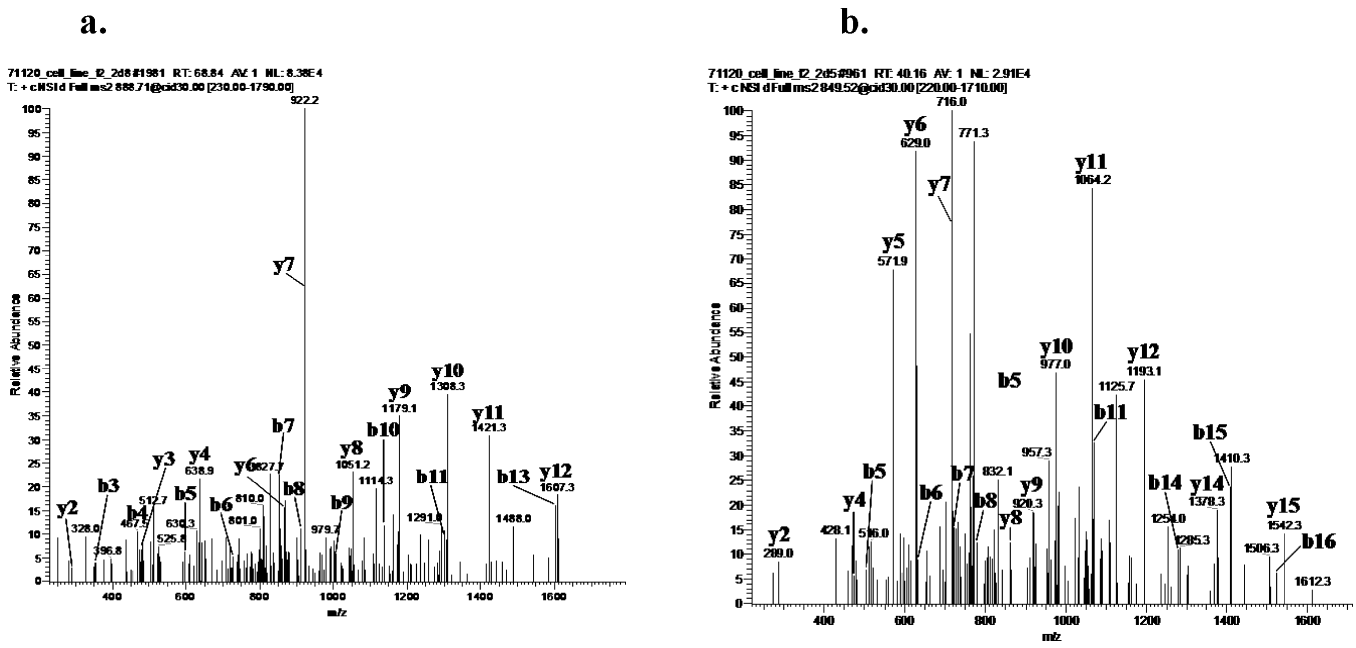

Figure 5. (a) The CID spectrum of a precursor ion *m/z* 888.7 $[M + 2H^+]^{2+}$ (t_r = 68.8 min in a salt step of 8 mM NH_4HCO_3) was matched with a peptide of R.APWIEQEGPEYWDR.N from *major histocompatibility complex, class I, B precursor* after a salt step elution with 8 mM NH_4HCO_3 and (b) MS-MS spectrum of R.APWIEQEGPEYWDR.N (*m/z* 849.6 $[M + 2H^+]^{2+}$, t_r = 40.2 min in a salt step of 5 mM NH_4HCO_3), which was identified as a peptide from *Ewing sarcoma breakpoint region 1 isoform EWS*.

Table 1. The Total Numbers of Proteins Identified by FI-AFlFFF and Ultracentrifugation Methods, and the Percentage of Membrane Proteins among All Identified Proteins in Each Fraction

	preparative method		
		fraction number from FI-AFlFFF	
localization	ultracentrifugation (UF)	fraction 1 (FF1)	fraction 2 (FF2)
Number of cytoplasmic proteins	141	127	93
Number of membrane proteins	127	55	154
Total	277	185	258
Percentage of membrane proteins	45.8	29.7	59.7

expected. The fractogram in Figure 3a also indicates that the intact cells were not disrupted or destroyed during the FI-AFlFFF run due to the flat baseline after the elution of cells.

Injection of cell lysate mixtures in the FI-AFlFFF run under the same conditions used in Figure 3 exhibited a significantly different elution pattern, which may have been due to presence of free cytoplasmic proteins, various subcellular species, and membrane fragments, all of which can be expected to elute at different retention time in accordance with their different sizes. Indeed, as shown in Figure 4, the fractogram of cell lysates (solid line) prepared by tip sonication appeared as a bimodal peak that eluted over a 10.0 min period under the same flow rate conditions used in Figure 3. When compared to the hyperlayer elution of intact DU145 cells shown in Figure 3, a mixed elution mode of separation (normal mode and hyperlayer mode) was expected, because the MWs of the majority of free cytoplasmic proteins released by lysis were less than 100 kDa and can thus be expected to run at normal mode (smaller one elutes earlier); however, membrane fragments after tip sonication will be much smaller than intact cells. To verify the elution pattern of the cell lysates, the pattern was superimposed with a fractogram of bovine serum albumin (BSA, 64.4 kDa), which was represented by the dotted lines in Figure 4, indicating that the first eluting peak was likely that of free proteins such as cytoplasmic ones. In principle, retention of proteins or even smaller nano-sized particles should elute with an increasing order of diameter due to their different diffusion coefficients acting against the channel wall. Thus, it was first assumed that the second eluting peak (from 3 to 10 min) represented the elution of much larger MW proteins or larger diameter cellular debris; however, based on our earlier experiments,[19,22,23] it appears that larger MW proteins (up to 670 kDa) require even higher crossflow rates than were used in this study (above 6 mL/min) in order to be successfully resolved from smaller molecules in the FI-AFlFFF channel. Therefore, the second peak was more likely originated from the elution of other nanometer-to-micrometer-sized species such as membrane fragments, undisrupted organelles, and biological vesicles. It was a possibility that target membrane fragments or debris could have been separated from most of cytoplasmic proteins by FI-AFlFFF, and indeed, this was validated later during identification of protein type and cellular localization.

Eluted lysates from FI-FlFFF runs were collected into two fractions (0 ~ 3 and 3 ~ 10 min of retention time). All fractions, including the two FI-FlFFF fractions (hereafter FF-1 and FF-2) and the ultracentrifugation fraction or pellets (hereafter UF), were cleaved enzymatically first with CNBr followed by trypsin. The resulting peptide mixtures were subsequently analyzed by online 2D-SCX-RPLC-MS-MS for protein identification. Peptide mixtures from each fraction were sequentially displaced from the SCX trap to the RP trap prior to the analytical column during the nine increasing salt (ammonium bicarbonate) concentration steps. After each salt displacement step, binary gradient separation using nLC-MS-MS was performed.

Table 2. Identification of Membrane Proteins and Their Cellular Location for Each Collected Fraction Using the Two Different Preparative Methods

					FlFFF	
gi number	protein name	cellular location	number of peptides matched	*UF	FF1	FF2
12025678	actinin, alpha 4	cell wall	4	v		v
113424511	actin-like protein	cell wall	3	v	v	v
55743080	ADAM metallopeptidase domain 2 proprotein	cell wall	1			v
28373192	adhesion regulating molecule 1 precursor	cell wall	1	v		
5453704	ADP-ribosylation-like factor 6 interacting protein 5	cell wall	2	v		
7705859	alpha-1,4-N-acetylglucosaminyltransferase	cell wall	1		v	
41406057	amyloid beta A4 protein precursor, isoform c	cell wall	1	v	v	
4557323	apolipoprotein C−III precursor	cell wall	2	v		v
68051721	arylacetamide deacetylase-like 1	cell wall	2	v		v
73486658	aspartate aminotransferase 2 precursor	cell wall	1			v
30795231	brain abundant, membrane attached signal protein 1	cell wall	4	v	v	v
38372931	brevican isoform 2	cell wall	2			v
4502549	calmodulin 2	cell wall	4	v	v	v
55770844	catenin, alpha 1	cell wall	2			v
91199546	CD63 antigen isoform B	cell wall	2		v	
24308201	chromosome 20 open reading frame 3	cell wall	2	v		v
65787364	coronin, Actin binding protein, 1B	cell wall	4	v	v	v
116534898	desmoglein 2 preproprotein	cell wall	2			v
34335253	disks large-associated protein 4 isoform a	cell wall	1		v	
4503571	enolase 1	cell wall	3	v		v
4885225	Ewing sarcoma breakpoint region 1 isoform EWS	cell wall	3	v	v	v
116063573	filamin A, alpha	cell wall	2	v		v
105990514	filamin B, beta (Actin binding protein 278)	cell wall	2	v		v
5031699	flotillin 1	cell wall	1			v
94538362	flotillin 2	cell wall	1			v
116805322	gamma filamin	cell wall	1	v		v
31377697	glycosyltransferase 25 domain containing 1	cell wall	2			v
118200356	growth hormone inducible transmembrane protein	cell wall	2	v		v
4504517	heat shock 27 kDa protein 1	cell wall	2	v	v	v
4885431	heat shock 70 kDa protein 1B	cell wall	1	v	v	
16507237	heat shock 70 kDa protein 5	cell wall	3	v	v	v
24234686	heat shock 70 kDa protein 8 isoform 2	cell wall	1			v
24234688	heat shock 70 kDa protein 9B precursor	cell wall	2	v	v	v
4758516	hepatoma-derived growth factor	cell wall	1	v		
116295258	integrin alpha 2 precursor	cell wall	4	v		v
4504747	integrin alpha 3 isoform a precursor	cell wall	1	v		v
19743815	integrin beta 1 isoform 1B precursor	cell wall	2	v		v
27777661	keratinocyte associated protein 2	cell wall	1			v
23308572	leukocyte receptor cluster (LRC) member 4 protein	cell wall	2			v
4505185	macrophage migration inhibitory factor	cell wall	1	v	v	
17986001	major histocompatibility complex, class I, B	cell wall	2	v		v
21536452	mesotrypsin preproprotein	cell wall	1		v	
23308607	minor histocompatibility antigen 13 isoform 1	cell wall	2	v		v
29568111	myosin regulatory light chain 9 isoform a	cell wall	2	v		v
5032223	plexin C1	cell wall	1		v	
45505137	podocan	cell wall	1			v
110224479	prosaposin isoform c preproprotein	cell wall	3	v	v	v
4506147	protease, serine, 2 preproprotein	cell wall	1		v	
59859885	ribosomal protein SA	cell wall	2	v		
16445421	secretory carrier membrane protein 3 isoform 2	cell wall	1			v
50659080	serpin peptidase inhibitor, clade A, member 3 precursor	cell wall	2	v	v	
88951501	similar to cytoplasmic beta-Actin	cell wall	2	v	v	v
4759112	solute carrier family 16, member 3	cell wall	2	v		v
112382252	spectrin, beta, nonerythrocytic 1 isoform 2	cell wall	1	v		v
126090466	spectrin, beta, nonerythrocytic 5	cell wall	1			v
5454052	stratifin	cell wall	1		v	
4507457	transferrin receptor	cell wall	3			v
13129092	transmembrane protein 109	cell wall	2	v		v
4502339	UDP-Gal:betaGlcNAc beta 1,3-galactosyltransferase 2	cell wall	1		v	
73466520	aldehyde dehydrogenase 3A2 isoform 1	ER	1			v
14589866	aspartate beta-hydroxylase isoform a	ER	1	v		v
24638454	ATPase, Ca^{2+} transporting, cardiac muscle, slow twitch 2 isoform 1	ER	2	v		v
66933005	calnexin precursor	ER	3	v		v

Table 2. Continued

gi number	protein name	cellular location	number of peptides matched	*UF	FlFFF FF1	FlFFF FF2
21361657	protein disulfide isomerase-associated 3 precursor	ER	2		v	v
4506675	ribophorin I precursor	ER	1			v
7019415	Sec61 alpha 1 subunit	ER	1		v	v
4507677	tumor rejection antigen (gp96) 1	ER	4		v	v
5803149	coated vesicle membrane protein	ER-golgi	2			v
5031973	protein disulfide isomerase-associated 6	ER-golgi	2			v
94429050	SEC22 vesicle trafficking protein homologue B	ER-Golgi	1			v
19557691	surfeit 4	ER-Golgi	2		v	v
9910280	UDP-glucose ceramide glucosyltransferase-like 1 isoform 1	ER-golgi	1			v
7705369	coatomer protein complex, subunit beta	golgi	1	v		v
18379349	vesicle amine transport protein 1	integral	1			v
17986283	tubulin, alpha 1a	intracellular	3	v		v
4501887	actin, gamma 1 propeptide	intracellular	2	v		v
4501891	actinin, alpha 1	intracellular	2	v		
5453595	adenylyl cyclase-associated protein	intracellular	1	v		
4501883	alpha 2 actin	intracellular	6	v	v	v
50845386	annexin A2 isoform 2	intracellular	4	v	v	v
4502101	annexin I	intracellular	1	v		
38372923	basigin isoform 4	intracellular	1			v
58535453	CDK5 regulatory subunit associated protein 2 isoform b	intracellular	1		v	
4758012	clathrin heavy chain 1	intracellular	4	v		v
4503583	epoxide hydrolase 1, microsomal (xenobiotic)	intracellular	2	v		v
4507943	exportin 1	intracellular	1			v
4826734	fusion (involved in t(12;16) in malignant liposarcoma) isoform a	intracellular	2	v		v
7669492	glyceraldehyde-3-phosphate dehydrogenase	intracellular	5		v	v
4557878	intercellular adhesion molecule 1 precursor	intracellular	1	v		v
24234756	interleukin enhancer binding factor 3 isoform c	intracellular	5	v		v
24234756	interleukin enhancer binding factor 3 isoform c	intracellular	4	v		v
4506787	IQ motif containing GTPase activating protein 1	intracellular	2	v		v
5730027	KH domain containing, RNA binding, signal transduction associated 1	intracellular	2			v
62868215	laminin subunit beta 3 precursor	intracellular	2	v		v
19718759	myoferlin isoform b	intracellular	2			v
15809016	myosin regulatory light chain MRCL2	intracellular	2	v		v
5453740	myosin regulatory light chain MRCL3	intracellular	3	v		v
41406064	myosin, heavy polypeptide 10, nonmuscle	intracellular	1			v
12667788	myosin, heavy polypeptide 9, nonmuscle	intracellular	3	v		v
17986258	myosin, light chain 6, alkali, smooth muscle and nonmuscle isoform 1	intracellular	2	v		v
41281987	nesprin 1 longest	intracellular	1	v		
154240744	neurobeachin-like 1 isoform 2	intracellular	1			v
4557803	Niemann-Pick disease, type C1	intracellular	1			v
24430149	nucleoporin 155 kDa isoform 1	intracellular	1	v		
58331253	obscurin, cytoskeletal calmodulin and titin-interacting RhoGEF	intracellular	1			v
150170670	piccolo isoform 2	intracellular	1		v	
41322908	plectin 1 isoform 3	intracellular	5	v		v
4758910	prostaglandin E synthase	intracellular	3	v		v
48255891	protein kinase C substrate 80K−H isoform 2	intracellular	2	v		
4506413	RAP1A, member of RAS oncogene family	intracellular	1	v		
4757768	Rho GDP dissociation inhibitor (GDI) alpha	intracellular	3	v		v
16579885	ribosomal protein L4	intracellular	3	v		v
11968182	ribosomal protein S18	intracellular	1	v		
17158044	ribosomal protein S6	intracellular	1	v		
5031631	scavenger receptor class B, member 2	intracellular	2	v		v
116256489	septin 9	intracellular	2	v		v
113429348	similar to 40S ribosomal protein S10	intracellular	1	v		v
89040395	similar to actin, alpha 2, smooth muscle, aorta	intracellular	2	v		
88943771	similar to melanoma inhibitory activity 3 isoform 2	intracellular	2			v
88992667	similar to myosin regulatory light chain-like	intracellular	2	v		v
4507191	spectrin, alpha, nonerythrocytic 1 (alpha-fodrin)	intracellular	2	v		v
7661952	squamous cell carcinoma antigen recognized by T cells 3	intracellular	4	v	v	v
7305503	stomatin (EPB72)-like 2	intracellular	2	v		v
16753233	talin 1	intracellular	4	v		v
48255913	tripartite motif-containing 16	intracellular	1		v	
5032179	tripartite motif-containing 28 protein	intracellular	2	v		v

Table 2. Continued

gi number	protein name	cellular location	number of peptides matched	*UF	FlFFF FF1	FlFFF FF2
47519616	tropomyosin 2 (beta) isoform 2	intracellular	1	v		
24119203	tropomyosin 3 isoform 2	intracellular	1	v		
14389309	tubulin alpha 6	intracellular	2	v		v
13376181	tubulin, alpha-like 3	intracellular	1			v
29788785	tubulin, beta	intracellular	3	v		v
29788768	tubulin, beta 2B	intracellular	3	v		v
29788785	tubulin, beta polypeptide	intracellular	4	v	v	v
5174735	tubulin, beta, 2	intracellular	1	v		
50592996	tubulin, beta, 4	intracellular	5	v		v
4759302	VAMP-associated protein B/C	intracellular	3	v		v
94721250	vesicle-associated membrane protein-associated protein A isoform 1	intracellular	2	v		
62414289	vimentin	intracellular	4	v		v
7669550	vinculin isoform meta-VCL	intracellular	3	v		v
4557231	acyl-Coenzyme A dehydrogenase, C-4 to C-12 straight chain	mitochondrial	1			v
6005717	ATP synthase, H+ transporting, mitochondrial F0 complex, subunit E	mitochondrial	1			v
4757810	ATP synthase, H+ transporting, mitochondrial F1 complex, alpha subunit	mitochondrial	4	v		v
32189394	ATP synthase, H+ transporting, mitochondrial F1 complex, beta subunit	mitochondrial	3	v		v
4502313	ATPase, H+ transporting, lysosomal, V0 subunit c	mitochondrial	2	v		v
115315571	Cytochrome *b*	mitochondrial	2	v		
11128019	cytochrome c	mitochondrial	2		v	v
58615666	cytochrome c oxidase subunit II	mitochondrial	5	v		v
17017988	cytochrome c oxidase subunit Vb precursor	mitochondrial	3	v		v
4502989	cytochrome c oxidase subunit VIIa polypeptide 2 (liver) precursor	mitochondrial	2	v		v
31711992	dihydrolipoamide S-acetyltransferase	mitochondrial	3	v		v
62530384	dodecenoyl-Coenzyme A delta isomerase precursor	mitochondrial	1	v		
52630440	FK506-binding protein 8	mitochondrial	1			v
41393575	glycerol kinase 2	mitochondrial	2		v	v
5803115	inner membrane protein, mitochondrial	mitochondrial	2	v	v	v
6912482	leucine zipper-EF-hand containing transmembrane protein 1	mitochondrial	2	v		v
31621305	leucine-rich PPR motif-containing protein	mitochondrial	1			v
22035634	microsomal glutathione S-transferase 1	mitochondrial	4	v	v	v
113422164	Mitochondrial import receptor subunit TOM22	mitochondrial	2	v		v
9910382	mitochondrial import receptor Tom22	mitochondrial	2	v	v	v
21735621	mitochondrial malate dehydrogenase precursor	mitochondrial	2		v	v
5174723	mitochondrial outer membrane protein TOM40	mitochondrial	1		v	v
34304322	mitochondrial ribosomal protein L45	mitochondrial	2		v	v
20127408	mitochondrial trifunctional protein, alpha subunit precursor	mitochondrial	2		v	v
4504327	mitochondrial trifunctional protein, beta subunit precursor	mitochondrial	5	v	v	v
4505241	Mpv17 protein	mitochondrial	1			v
4826852	NADH dehydrogenase (ubiquinone) 1, alpha/beta subcomplex, 1, 8 kDa	mitochondrial	2	v		v
58615663	NADH dehydrogenase subunit 1	mitochondrial	2		v	v
122939153	nicotinamide nucleotide transhydrogenase	mitochondrial	2	v	v	v
4557809	ornithine aminotransferase precursor	mitochondrial	2	v	v	v
4506649	ribosomal protein L3 isoform a	mitochondrial	2	v	v	v
23618867	sideroflexin 1	mitochondrial	3	v	v	v
31621303	sideroflexin 3	mitochondrial	3	v	v	v
55749577	solute carrier family 25	mitochondrial	3	v	v	v
4505775	solute carrier family 25 member 3 isoform b precursor	mitochondrial	2	v		v
4502099	solute carrier family 25, member 5	mitochondrial	3	v		v
27764863	solute carrier family 25, member 6	mitochondrial	2	v		v
6912714	translocase of inner mitochondrial membrane 9 homologue	mitochondrial	1	v		v
7657257	translocase of outer mitochondrial membrane 20 homologue	mitochondrial	1			v
34147630	Tu translation elongation factor, mitochondrial	mitochondrial	2	v	v	v
113416816	Ubiquinol-cytochrome c reductase complex 14	mitochondrial	3	v		
46593007	ubiquinol-cytochrome c reductase core protein I	mitochondrial	2	v		
50592988	ubiquinol-cytochrome c reductase core protein II	mitochondrial	3	v		v
4507879	voltage-dependent anion channel 1	mitochondrial	1	v		v
70166944	adenosine deaminase, RNA-specific isoform b	nucleus	3	v		v
62460637	importin 4	nucleus	2			v

Table 2. Continued

gi number	protein name	cellular location	number of peptides matched	*UF	FlFFF FF1	FlFFF FF2
5453998	importin 7	nucleus	1			v
32455256	LAG1 longevity assurance homologue 2	nucleus	2	v		v
21626466	matrin 3	nucleus	3	v		v
4757886	pituitary tumor-transforming gene 1 protein-interacting protein precurs	nucleus	1		v	
6466466	RAN binding protein 3 isoform RANBP3-d	nucleus	3		v	
115334679	retinoblastoma-binding protein 1 isoform III	nucleus	1		v	
73760401	thymopoietin isoform gamma	nucleus	2	v		v
4507357	transgelin 2	nucleus	2	v		v
21361320	TRK-fused	nucleus	1			v

Figure 5a shows the collision induced dissociation (CID) spectrum of a precursor ion m/z 888.7 $[M + 2H^+]^{2+}$ detected at retention time of 68.8 min during the nLC-MS run of the digested peptide sample from FF2 (FFF fraction number 2), which was run immediately after the salt step elution with 8 mM NH_4HCO_3. A Chromatogram of the nLC run was not included here. A search against a human database produced information regarding a peptide with the sequence R.APWIEQEGPEYWDR.N, which was derived from *major histocompatibility complex, class I, B precursor*. This protein is known to be localized at the cell membrane, where it is reported to play an important role in the immune system of healthy cells by presenting peptides derived from the endoplasmic reticulum lumen.[24,25] In addition, Figure 5b shows the MS-MS spectrum of a precursor ion m/z 849.6 $[M + 2H^+]^{2+}$, which was detected at $t_r = 40.2$ min in a salt step of 5 mM NH_4HCO_3, of which a database search produced a match with the peptide R.APWIEQEGPEYWDR.N which originates from *Ewing sarcoma breakpoint region 1 isoform EWS*. This protein is also known to localize at the cell membrane, where it is reported to cause Ewing sarcoma, a well-documented neuroectodermal tumor, along with various other tumor types.[26−28]

On the basis of the 2D-SCX-LC-MS-MS analysis of each fraction, a total of 185 and 258 proteins were identified from the FF1 and FF2 fractions, respectively, while 277 proteins were identified from the UF fraction. In particular, the numbers of proteins classified as membrane proteins, including subcellular membrane proteins, were 55 for FF1, 154 for FF2, and 127 for UF, as listed in Table 1. These numbers include proteins that localize to the cell membrane as well as from subcellular membranes of the nucleus, mitochondria, endoplasmic reticulum, and golgi. The relative coverage of membrane proteins among the total number of proteins identified at each fraction corresponded to 59.7% for FF2 and 45.8% for UF fraction, indicating that the second fraction from FI-AFlFFF provided a higher yield of isolated membrane proteins compared to the ultracentrifugation method. Unlike the FF2 and UF fractions, the FF1 fraction had a relatively lower yield of membrane proteins, at 29.7%, which may have originated from smaller sized membrane fragments that coeluted with the cytoplasmic proteins.

The membrane proteins identified from the three fractions are listed in Table 2, and are sorted by their cellular localization. Overall, 172 proteins were classified as membrane proteins from both the FI-AFlFFF fractions 1 and 2, whereas only 127 were classified using the ultracentrifugation method. This result was due to the fact that FF2 contained more membrane proteins from subcellular structures such as the nucleus, mitochondria, endoplasmic reticulum, and golgi as well as membrane fragments of cell wall, compared to the ultracentrifugation fraction. In addition to these results, we also observed that FI-AFlFFF was associated with a decreased chance of losing biological vesicles and disrupting subcellular membranes, which are often difficult to retrieve by ultracentrifugation alone.

Conclusion

FI-AFlFFF was employed to purify both membrane fragments and membrane proteins from whole cell lysates of DU145 cells with depletion of cytoplasmic proteins. On the basis of our proteomic analysis, it was found that the FI-AFlFFF could be successfully utilized as a soft preparative method that is more suitable than ultracentrifugal preparation techniques for isolating target membranes from cell lysates and for minimizing the loss of subcellular vesicles. In addition, FI-AFlFFF had several other merits, including the ability to collect membrane fragments without aggregation due to pelleting, online monitoring of yield by using a detector signal, and the significant reduction of the separation time, which is about 10∼12 min for each run, while ultracentrifugation requires 1 h for each step and needs repeated purifications. While the current study did not demonstrate a complete isolation of membrane fragments from subcellular species, it is a promising possibility that subcellular species may be successfully fractionated through further optimization of the separation conditions. Despite its limitation, FI-AFlFFF appears to be a powerful new alternative to traditional centrifugal methods that can enhance the yield of purified membrane proteins.

Acknowledgment. This work was supported by KBSI grant T2823A to PI HSK and partly by a grant (2008-03136) from the Korea Ministry of Science & Technology (MOST).

References

(1) Walmsley, A. R.; Zeng, F.; Hooper, N. M. *EMBO J.* **2001**, *20*, 703–712.
(2) Spinazzola, A.; Viscomi, C.; Fernandez-Vizarra, E.; Carrara, F.; D'Adamo, P.; et al. *Nat. Genet.* **2006**, *38*, 570–575.
(3) Yanagisawa, K.; Odaka, A.; Suzuki, N.; Ihara, Y. *Nat. Med.* **1995**, *1*, 1062–1066.
(4) Xiang, R.; Shi, Y.; Dillon, D. A.; Negin, B.; Horvath, C.; Wilkins, J. A. *J. Proteome Res.* **2004**, *6*, 1278–1283.
(5) Fischer, F.; Wolters, D.; Rögner, M.; Poetsch, A. *Mol. Cell. Proteomics* **2006**, *5*, 444–453.
(6) Fischer, F.; Wolters, D.; Rögner, M.; Poetsch, A. *J. Proteome Res.* **2002**, *1*, 351–360.
(7) Zhao, Y.; Zhang, W.; Kho, Y.; Zhao, Y. *Anal., Chem.* **2004**, *1*, 1817–1823.
(8) Pretlow, T. G.; Pretlow, T. P. *Nature* **1988**, *333*, 97–97.
(9) Wldhalm, K.; Pakosta, R. *Clin. Chem.* **1991**, *37*, 238–240.
(10) Giddings, J. C. *Anal. Chem.* **1981**, *53*, 1170A–1175A.

(11) Reschiglian, P.; Zattoni, A.; Roda, B.; Cinque, L.; Mellucci, D.; Min, B. R.; Moon, M. H. *J. Chromatogr., A* **2003**, *985*, 519–529.
(12) Moon, M. H.; Kim, Y. H.; Park, I. *J. Chromatogr., A* **1998**, *813* (1), 91–100.
(13) Kang, D.; Oh, S.; Ahn, S.-M.; Lee, B.-H.; Moon, M. H. *J. Proteome Res.* **2008**, *7* (8), 3475–3480.
(14) Kang, D.; Oh, S.; Reschiglian, P.; Moon, M. H. *Analyst* **2008**, *133*, 505–515.
(15) Oh, S.; Kang, D.; Ahn, S.-M.; Simpson, R. J.; Lee, B.−H.; Moon, M. H. *J. Sep. Sci.* **2007**, *30*, 1982–1087.
(16) Giddings, J. C. *Science* **1993**, *260*, 1456–1465.
(17) Stone, K. R.; Mickey, D. D.; Wunderli, H.; Mickey, G. H.; Paulson, D. F. *Int. J. Cancer* **1978**, *21*, 274–281.
(18) Moon, M. H.; Kwon, H.; Park, I. *Anal. Chem.* **1997**, *69* (9), 1436–1440.
(19) Moon, M. H.; Williams, P. S.; Kwon, H. *Anal. Chem.* **1999**, *71* (14), 2657–2666.
(20) Kang, D.; Nam, H.; Kim, Y.-S.; Moon, M. H. *J. Chromatogr., A* **2005**, *1070*, 193–200.
(21) Bang, D. Y.; Ahn, E.; Moon, M. H. *J. Chromatogr., B* **2007**, *852*, 268–277.
(22) M., H.; Hwang, I. *J. Liq. Chromatogr. Relat. Technol.* **2001**, *24* (20), 3069–3083.
(23) Park, I.; Paeng, K.−J.; Yoon, Y.; Song, J.−H.; Moon, M. H. *J. Chromatogr., B* **2002**, *780*, 415–422.
(24) Fabian, H.; Huser, H.; Narzi, D.; Misselwitz, R.; Loll, B.; Ziegler, A.; Bockmann, R. A.; Uchanska-Ziegler, B.; Naumann, D. *J. Mol. Biol.* **2008**, *376* (3), 798–810.
(25) Nejentsev, S.; Howson, J. M.; Walker, N. M.; Szeszko, J.; Field, S. F. *Nature* **2007**, *450* (7171), 887–892.
(26) Potikyan, G.; Savene, R. O.; Gaulden, J. M.; France, K. A.; Zhou, Z. *Cancer Res.* **2007**, *67* (14), 6675–6684.
(27) Delattre, O.; Zucman, J.; Plougastel, B.; Desmaze, C.; Melot, T. *Nature* **1992**, *359* (6391), 162–165.
(28) Ohno, T.; Ouchida, M.; Lee, L.; Gatalica, Z.; Rao, V. N.; Reddy, E. S. *Oncogene* **1994**, *9* (10), 3087–3097.

PR800689Y